A Two-Component Model for the Phase Behavior of Dispersions Containing Associative Polymer

Maria M. Santore, William B. Russel,* and Robert K. Prud'homme

Department of Chemical Engineering, Princeton University, Princeton, New Jersey 08544.
Received May 10, 1988; Revised Manuscript Received August 22, 1988

ABSTRACT: A statistical mechanical theory is developed to predict the flocculation or phase separation of a colloidal dispersion by associating polymer. The system is modeled as a binary mixture of hard colloid spheres and Gaussian polymer chains with adhesive end groups or "stickers". Interaction potentials are derived in terms of the sticker–sticker and sticker–colloid adhesion energies and the number of Gaussian segments in a coil. These pair potentials then determine equilibrium phase behavior via the Barker–Henderson perturbation theory. Phase diagrams illustrate the effects of polymer properties on the extent of fluid–fluid phase separation. In the weak sticker limit, volume restriction flocculation is predicted; however, increasing sticker–colloid adhesion stabilizes the system.

Introduction

Colloidal dispersions containing dissolved polymer exhibit different equilibrium phase behavior depending on the interaction between the particles and polymer molecules. For example, nonadsorbing polymer in high concentrations can cause volume restriction flocculation,[1] while small amounts of randomly adsorbing polymer can induce bridging flocculation.[2] Associating polymer, which adsorbs to the particles at specific points along the backbone, can suppress both phenomena.[3]

Polymer is added to colloidal dispersions to regulate their physical properties. Depending on the particular application, bridging flocculation, volume restriction flocculation, or stabilization may be desired. In the paint industry, nonadsorbing water-soluble polymer, such as (hydroxyethyl)cellulose, is added to stable colloidal dispersions to increase the viscosity via a volume restriction flocculation mechanism.[3-5] Polymer molecules are excluded from a region close to the particle surface. When the exclusion layers of two particles overlap, polymer molecules cannot penetrate the gap. The polymer concentration difference between the bulk solution and the gap generates an osmotic force which drives the particles together. This attractive potential becomes comparable to the thermal energy of the particles and capable of producing a phase separation, in the form of volume restriction flocculation, at modest polymer concentrations. In conventional paints, microphase separation imparts a yield stress which translates into very high viscosities at low shear rates and dramatic shear thinning behavior, neither of which are desirable paint qualities.

A desire to improve rheological properties led to the development of associative thickeners,[6] water-soluble polymers containing 1–2 wt % hydrocarbon branches (8–18 carbons long) which associate weakly and adsorb reversibly onto hydrophobic surfaces such as latex spheres. An example, hydrophobically modified (hydroxyethyl)cellulose[7,8] has a relatively high molecular weight (~250 kg/mol) linear backbone along which hydrocarbon arms are distributed. Polyurethane thickeners[9] of typically lower molecular weight (~75 kg/mol) contain hydrophobic end groups thought to be primarily responsible for their associative nature. The polyurethane thickener may also contain regularly spaced internal hydrophobes between long polyether chains. Both types of polymers are attractive alternatives to conventional thickeners because they provide additional degrees of freedom for controlling dispersion properties. The largest deterrent to their widespread use has been a lack of understanding of the influence of polymer characteristics on dispersion properties.

Apparently, a modified polymer must be tailored for a specific dispersion. For example, associative polymer can stabilize latices or cause bridging flocculation.[3] At conditions which minimize the associative affects of the hydrophobe, these polymers also induce volume restriction flocculation.[3] Clearly, the equilibrium behavior of these systems is complex and poorly understood, as are their rheological properties. Equilibrium phase behavior is fundamentally important as an aid in characterizing such dispersions, and as the first step toward understanding their flow behavior. Appropriately, this paper proposes a theory describing the effects of associative interactions on the equilibrium phase behavior of colloidal dispersions.

Previous attempts to model colloidal dispersions containing dissolved polymer integrated the effects of polymer and solvent into the interparticle potential.[4,10-12] This "pseudo-one-component" approach presumes that an effective colloid–colloid interaction potential alone dictates the properties of the system. The important thermodynamic variables, then, are particle volume fraction and polymer concentration. The latter is equivalent to the inverse temperature since it establishes the strength of the particle–particle attraction. The criteria for phase equilibria are equal colloid chemical potentials and pressures in all phases. Implicit in this approach is the assumption that the polymer concentration in the fluid around the particles is equal in all phases.

Sperry[10] used this pseudo-one-component approach to calculate colloid–colloid potentials, including an osmotic attraction which favors volume restriction flocculation and an electrostatic repulsion which acts to stabilize the system. Comparison with experimental data indicated phase separations when the attractive minimum in the colloid–colloid interaction potential became −2.7 kT or greater. However, the theory neither forecasted the compositions of the resulting phases nor distinguished between fluid–solid and fluid–fluid transitions.

The statistical mechanical treatment of Gast et al.[4,11,12] also depends on the pseudo-one-component approach. The polymer-induced attraction in the colloid–colloid pair potential was incorporated through the Barker–Henderson perturbation theory to predict macroscopic properties such as Helmholtz free energy. Application of the thermodynamic criteria for phase equilibria in a single-component system led to phase diagrams identifying single- and two-phase regions in particle volume fraction (concentration) and polymer concentration (temperature) space. Both fluid–fluid and fluid–solid equilibria were predicted, depending on the ratio of particle to polymer size.

An alternative, the pseudo-two-component approach, treats the polymer-containing colloidal dispersion as a

0024-9297/89/2222-1317$01.50/0

binary mixture of particles and polymer molecules. The effects of the solvent are implicit in the polymer–polymer, polymer–colloid, and colloid–colloid interaction potentials. Phase equilibrium is determined by the classical thermodynamic criteria for binary mixtures: equality of pressure, colloid chemical potential, and polymer chemical potential in all phases. Particle and polymer volume fractions determine the thermodynamic variables and, hence, the state of the system.

The pseudo-two-component or binary mixture approach is exemplified by Melnyk and Sawford's[13] perturbation theory for a nonadditive hard sphere mixture, e.g., two species of the same size but with cross interactions having a larger excluded volume than the like interactions. In this case, nonadditivity causes a fluid–fluid phase separation with a critical point at a mole fraction of 0.5. Melnyk and Sawford confirmed the accuracy of their perturbation theory with a Monte Carlo simulation. The concept that nonadditivity induces fluid–fluid phase separations is important, and Melnyk and Sawford's approach can be extended to systems of different sized spheres.

Our treatment of dispersions containing associative polymer implements a pseudo-two-component approach, based on the colloid–colloid, polymer–polymer, and polymer–colloid interaction potentials. The polymer–polymer and polymer–colloid potentials are derived in the spirit of Cates and Witten[14] for a Gaussian chain with stickers, treated as δ functions, on either end. This approach greatly simplifies the mathematics. The interaction potentials, together with the Barker–Henderson perturbation theory[15,16] for mixtures, yield the Helmholtz free energy as a function of the particle and polymer volume fractions. Phase diagrams of the fluid–fluid transition are generated for binary mixtures. This theory assumes random walk statistics for the chains, stickers which act as δ functions with no volume, and polymer molecules significantly smaller than the particles.

In the next section, we derive the various interaction potentials and discuss their implications for phase behavior. The Barker–Henderson perturbation theory is then outlined. Finally, we describe our procedure for generating phase diagrams and discuss the predicted effects of associative polymer on the phase behavior of colloidal dispersions.

Pair Potentials

In this section, we derive the pair potentials which lie at the heart of the statistical mechanical treatment of the polymer–particle system. The colloid–colloid hard sphere interaction is trivial, but the polymer–polymer and polymer–colloid potentials require a detailed model of the polymer molecules to account for both the internal degrees of freedom and the associative hydrophobes. For simplicity, we model the polymer as a Gaussian chain with a sticker at either end. The random walk character of the polymer implies that excluded volume interactions have been neglected. Each chain consists of N Gaussian segments of step length l, with u_{pp} and u_{pw} denoting the adhesion energies for sticker–sticker and sticker–colloid contacts, respectively. The polymer–polymer and polymer–particle potentials are calculated from the configurational integral, which requires a knowledge of the statistics of the backbone.

The polymer statistics can be derived from the diffusion equation,

$$\frac{\partial P(s,\mathbf{R}|\mathbf{0})}{\partial s} = \frac{l^2}{6}\nabla^2 P(s,\mathbf{R}|\mathbf{0}) \tag{1}$$

$P(s,\mathbf{R}|\mathbf{0})$ is the probability distribution function, i.e., the probability of finding the sth segment at position $\mathbf{R}$ if the first segment is at $\mathbf{0}$. When eq 1 is solved with the boundary condition that the probability of finding a segment at infinity is vanishingly small, one obtains the classical Gaussian segment distribution,[17]

$$P(s,\mathbf{R}|\mathbf{0}) = \left(\frac{2}{\pi^{1/2}}\right)^3\left(\frac{3}{2l^2s}\right)^{3/2}\exp\left(\frac{-3}{2l^2s}R^2\right) \tag{2}$$

describing the configurations of a polymer chain in isolation.

The theory also requires the configuration of the polymer near a particle. Solving the diffusion equation with boundary conditions on the particle surface is difficult; however, for polymer molecules much smaller than the particle, the interaction resembles that with a wall. The corresponding polymer configuration near a wall at $x = 0$ is obtained by solving eq 1 with the additional boundary condition that the probability vanishes for $x \le 0$. The probability density for a polymer with one end at (x',y',z'), the other end at $(x,0,0)$, and no segments beyond a wall at $x = 0$ results:[18]

$$P(s,x,y,z|x',0,0) = \left(\frac{2}{\pi^{1/2}}\right)^3\left(\frac{3}{2l^2s}\right)^{3/2}\exp\left(\frac{-3}{2l^2s}(y^2+z^2)\right)\times\left\{\exp\left(\frac{-3}{2l^2s}(x-x')^2\right)-\exp\left(\frac{-3}{2l^2s}(x+x')^2\right)\right\} \tag{3}$$

Note that the stickers do not enter into the probability distribution functions, but play a role in the configurational integral below.

Equations 2 and 3 suffice to calculate the configurational integral of two polymers in solution or that of a polymer near an infinite wall. The configurational integral simplifies because the stickers act as δ functions in space, associating an energy only with those configurations where the stickers adhere to each other with adhesion energy u_{pp}/kT, or to the wall with adhesion energy u_{pw}/kT. Hence the polymer–polymer and polymer–wall (or particle) configurational integrals become

$$W_{pp} = 1 + W_1(R)(e^{-u_{pp}/kT}-1) + W_2(R)(e^{-2u_{pp}/kT}-1) + W_3(R)(e^{-3u_{pp}/kT}-1) + W_4(R)(e^{-4u_{pp}/kT}-1) \tag{4a}$$

where R is the distance between the middle segments (i.e., segment number $N/2$) of the two chains, and $W_i(R)$ is the probability that two chains of N Gaussian segments have i sticker–sticker contacts. The polymer–wall configurational integral becomes

$$W_{pw} = W_0^{w}(R) + W_1^{w}(R)(e^{-u_{pw}/kT}-1) + W_2^{w}(R)(e^{-2u_{pw}/kT}-1) + W^{w}{}_{0loop}(R)(e^{-u_{pp}/kT}-1) + W^{w}{}_{2loop}(R)(e^{(-2u_{pw}-u_{pp})/kT}-1) \tag{4b}$$

where R is the distance between the middle segment of the polymer and the wall, $W_0^{w}(R)$ is the fraction of configurations available to a polymer constrained to be a distance R from the wall, $W_i^{w}(R)$ is the probability that a chain of N Gaussian segments has i ends adsorbed (at a distance $l/2$ from the wall), and $W^{w}{}_{iloop}(R)$ is the probability of a loop with i ends adsorbed. The configurational integrals are normalized on a bulk solution where the polymer may assume a ring configuration.

All $W_i(R)$ and $W_i^{w}(R)$ are calculated from (2) and (3) with the distance R between two chains or between the chain and the wall based on the position of the middle segment (i.e., segment number $N/2$). In calculating these probabilities for the various configurations of contacting chains, we multiply probabilities for half chains, specify

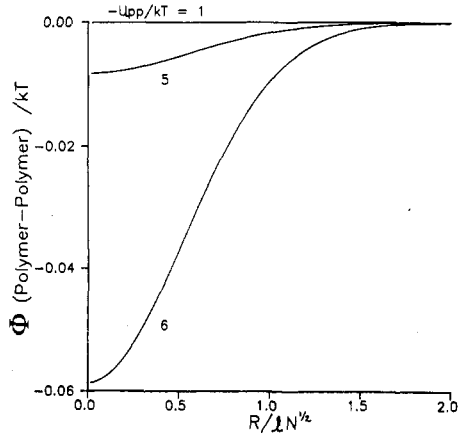

Figure 1. Effect of sticker–sticker adhesion on the polymer–polymer potential: $N = 1000$.

the position of the adsorbed ends, and integrate the positions of free ends over all available space. For example, a single polymer–wall contact has the midsegment at (R,y,z), the adsorbed end at $(l/2,y'',z'')$, and the free end at (x',y',z'). Using the Gaussian probability from eq 3, we calculate $W_1^w(R)$ as

$$W_1^w(R) = \int \dots \int P(N/2,l/2,y'',z''|R,y,z) \times P(N/2,R,y,z|x',y',z')\, dy\, dz\, dx'\, dy'\, dz'\, dy''\, dz'' \quad (5)$$

where all y and z variables integrate from $-\infty$ to ∞ and dx' integrates from 0 to ∞.

The interaction potentials follow from the configurational integrals as the work to move polymers or particles and polymers together, i.e., the change in Helmholtz free energy. Hence, we find the polymer–polymer and polymer–wall potentials to be

$$\Phi_{pp}(R) = -kT \ln (W_{pp}(R))$$
$$\Phi_{pw}(R) = -kT \ln (W_{pw}(R)) \quad (6)$$

Because the configurational integrals are normalized, they approach unity at infinite separation, giving an interaction potential of zero at infinity.

The polymer–polymer and polymer–particle interaction potentials depend on three parameters, u_{pp}, u_{pw}, and N, and provide insight into the macroscopic properties of the system. The sticker–sticker adhesion primarily affects the polymer–polymer potential, with a lesser effect on the polymer–colloid potential through the reference state. Figure 1 shows the general shape of the polymer–polymer potential with an attractive minimum at zero separation and no repulsive core because the polymer is assumed ideal. As u_{pp} increases in magnitude from $-kT$ to $-6kT$, the attractive well becomes deeper and more long range but remains less than $0(0.1kT)$ while the polymer solution is soluble, as determined by the stability analysis in the next section.

Also of interest is the fraction of stickers that are paired in bulk solution. When all the stickers are paired, the number of sticker pairs equals the number of polymer molecules, since each has two stickers. Simple calculations show that, for $u_{pp} = O(kT)$, this will occur near the polymer overlap concentration. In general, the requisite sticker–sticker energy is inversely proportional to volume fraction, since entropy favors uncoupled stickers.

The shape of the polymer–wall potential reflects the competing effects of entropic repulsion and sticker–wall adhesion, as shown in Figure 2. The repulsive core results from the loss of configurational entropy of a polymer chain constrained to lie close to a flat surface. As the sticker–wall

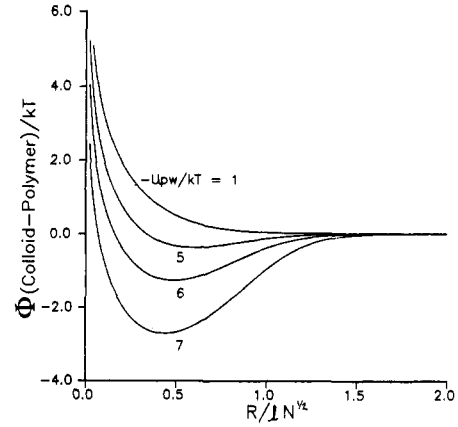

Figure 2. Effect of sticker–wall adhesion on the colloid–polymer potential: $N = 1000$, $u_{pp}/kT = -1$.

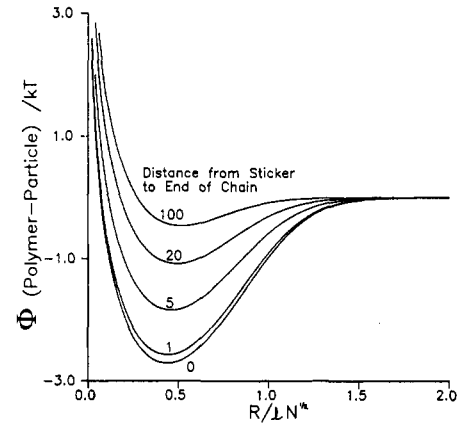

Figure 3. Effect of sticker position on the colloid–polymer potential: $N = 1000$ total, $u_{pw} = -7kT$, $u_{pp} = -kT$.

adhesion increases, an attractive well appears in the interaction potential. For $u_{pw} = -6kT$, the depth of the attractive well is $O(kT)$, 1–2 orders of magnitude greater than the corresponding attraction in the polymer–polymer potential. Increasing the sticker–wall adhesion also moves the minimum closer to the wall because strong adhesion increases the probability that the polymer has both ends adhering to the wall. From the graph, it is difficult to discern the sticker–wall adhesion at which the attraction first appears; however, the numerical results clearly indicate attractive wells for $u_{pw} \leq -2.7kT$.

In addition to sticker strength, many polymer characteristics such as sticker placement, chain flexibility, and backbone topology determine interaction potentials. Figure 3 shows that, as the stickers are moved inward from the ends of the chain, the polymer–particle potential becomes less attractive. The additional branch beyond the sticker impedes adhesion to the surface; hence, the sticker gets lost within the polymer coil.

Figure 4 shows the effect of branching on the polymer–particle potential, exemplified by increasing the number of arms (only two of which have stickers) in a star-shaped polymer but maintaining a constant total segment number. Increasing the number of arms compacts the polymer, as is evident by the decreased range of the repulsion and the position of the attractive well. Coils with more arms are more strongly attracted to the surface because shorter arms increase the probability of sticker–wall contact.

Sticker position and arm number do not directly affect the polymer–polymer potential. Sticker–sticker adhesion (Figure 1) and the number of segments between stickers (Figure 5) are the key polymer characteristics to influence

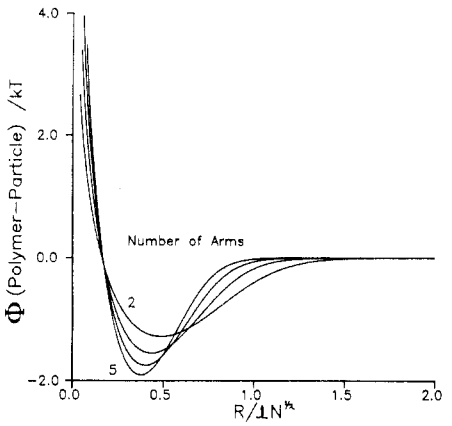

Figure 4. Effect of increasing the number of arms in a star polymer on the polymer–particle potential. (Only two arms contain stickers.) $N = 1000$ total, $u_{pw} = -6kT$, $u_{pp} = -kT$.

this potential. Because the polymer is ideal, additional branches from the midsegment and fragments beyond the sticker do not influence the interaction between two polymer molecules.

The number of Gaussian units affects both the polymer–polymer and polymer–colloid potentials. One may interpret N as a measure of either polymer size or flexibility because an infinite wall provides no length scale by which to measure polymer size. Figure 5 shows that, as N is decreased, both potentials become more attractive. There are two reasons for this effect. First, the configurational entropy in the polymer–particle potential becomes larger as N increases. Second, the Gaussian statistics are dominated by a $N^{-3/2}$ term which makes it less likely that a long or flexible polymer will have a sticker–sticker or sticker–wall contact.

The shape of the potential profoundly affects the phase behavior of the system. In a binary mixture, the phase separation is driven by two affects: the attraction between polymer molecules and the nonadditivity of repulsive cores. A highly nonadditive hard sphere mixture, such as ours when the sticker adhesions are weak, will phase separate because like species can approach each other more closely than unlike species. In other words, the additional distance between unlike species can be considered a repulsion which drives a phase separation. Attraction between polymer molecules also favors destabilization since the separated system not only packs more efficiently, but has less internal energy. Increasing the sticker–wall adhesion, however, produces an attraction between unlike species which should eventually overcome nonadditivity, maintaining a single-phase system.

Perturbation Theory

In order to calculate the conditions for phase equilibrium, one must have expressions for macroscopic thermodynamic variables such as the Helmholtz free energy. Perturbation theory facilitates calculating macroscopic properties from interaction potentials. The crux of perturbation theory[19] is to decompose the pair potentials into a short-range repulsion for the reference state and an attractive perturbation. For liquids this representation is fairly accurate because short-range repulsions primarily determine structure, while the longer range attractions provide a background that holds the liquid together. Some perturbation theories are single component, others treat mixtures by perturbing about either a single-component or a mixed reference state.

In the Barker–Henderson perturbation theory for a multicomponent Lennard-Jones fluid,[15] the Helmholtz free

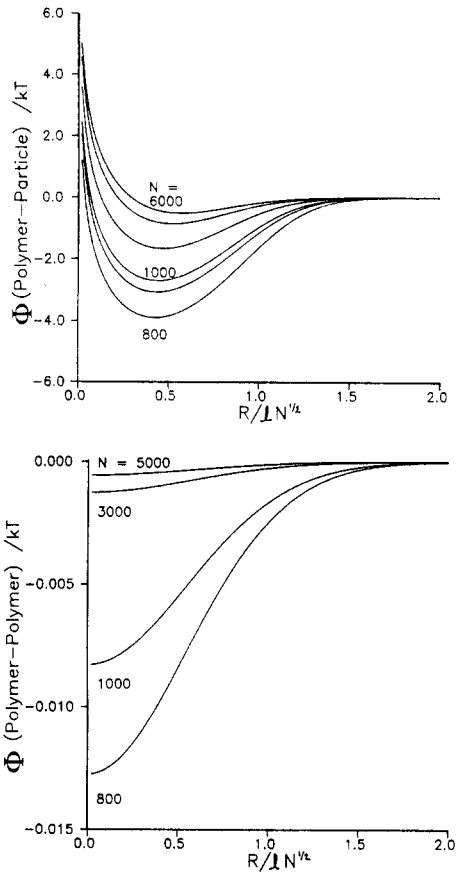

Figure 5. Effect of the number of Gaussian segments on (A, top) colloid–polymer ($u_{pw} = -7kT$, $u_{pp} = -kT$) and (B, bottom) polymer–polymer ($u_{pw} = -kT$, $u_{pp} = -5kT$) interaction potentials.

energy is expanded in a double perturbation in terms of γ, the depth of the attractive well, and $1/\alpha$, the steepness of the repulsion. This requires expressing the interactive potentials such that they reduce to those of a hard sphere mixture when γ and α vanish. To meet these requirements, a modified pair potential, v_{ij}, is defined in terms of the actual potentials, Φ_{ij}, calculated in the previous section,

$$\exp[-\beta v_{ij}(R)] = \left(1 - H\left[d_{ij} + \frac{R - d_{ij}}{\alpha_{ij}} - \sigma_{ij}\right]\right) \times \exp\left(-\beta\Phi_{ij}\left(d_{ij} + \frac{R - d_{ij}}{\alpha_{ij}}\right)\right) + H\left[d_{ij} + \frac{R - d_{ij}}{\alpha_{ij}} - \sigma_{ij}\right] + H(R - \sigma_{ij})(\exp[-\gamma_{ij}\beta\Phi_{ij}(R)] - 1) \quad (7)$$

where H is the Heaviside step function and d_{ij} is an effective reference diameter. Here, σ_{ij} is the point where Φ_{ij} passes through zero. The potential, v_{ij}, is independent of d_{ij} and reduces to $\Phi_{ij}(r)$ when $\gamma_{ij} = \alpha_{ij} = 1$. Conversely, when $\alpha_{ij} = \gamma_{ij} = 0$, $v_{ij}(r)$ is the multicomponent hard sphere potential which forms the reference state for this theory. Expanding the Helmholtz energy in γ_{ij} and α_{ij} eventually leads to

$$\frac{A - A^\circ}{kT} = -\sum_{ij} 2\pi\alpha_{ij}\rho d_{ij}^2 g^\circ_{ij}(d_{ij})(d_{ij} - \delta_{ij}) + 2\pi\rho\beta\sum_{ij}\gamma_{ij}x_i x_j \int_0^\infty \Phi_{ij}(R) g^\circ_{ij}(R) R^2\, dR + O(\alpha^2) + O(\alpha\gamma) + O(\gamma^2) \quad (8)$$

where A° is the free energy of the reference state, g°_{ij} the radial distribution function for the reference state, x_i and x_j the mole fractions of the two species, and

$$\delta_{ij} = \int_0^{\sigma_{ij}} (1 - e^{-\beta\Phi_{ij}(R)})\, dR \quad (9)$$

A hard sphere reference state with diameters d_{ij} of

$$d_{ij} = \delta_{ij} \quad \text{if} \quad i = j \quad (10a)$$

cancels two terms in the first summation of eq 8 and predetermines

$$d_{12} = (d_{11} + d_{22})/2 \quad (10b)$$

so that $d_{12} \neq \delta_{12}$. Equation 10 comprises an "additive" hard sphere system, leaving the $i = 1, j = 2$ term in the first summation of eq 8 to describe the nonadditivity. That is, in the reference state, cross-interactions are determined by the same collision diameters as the like interactions, while in the real system the cross-interactions have a larger diameter; i.e., $\delta_{12} > d_{12}$. The second term of eq 8 corrects for the attractive portion of the actual interaction potential.

Hard Sphere Reference State. Mixtures of hard spheres are described by the Carnahan–Starling equation of state,[20] which obtains excellent agreement with Monte Carlo simulations by combining the compressibility and pressure equations from the Percus Yevick approximation. When the equivalent diameter of the polymer vanishes, as it does in (9) above, the reference mixture compressibility and Helmholtz free energy simplify to

$$Z = \frac{P}{\rho kT} = [1 + (1 - 3x_p)\phi_c + \phi_c^2 + (x_p - 1)\phi_c^3](1 - \phi_c)^{-3} \quad (11a)$$

and

$$A - A^I = (1 - x_p)\phi_c(4 - 3\phi_c)(1 - \phi_c)^{-2} - x_p \ln (1 - \phi_c) \quad (11b)$$

where A^I is the ideal Helmholtz free energy, x_p is the number or mole fraction of polymer ($x_p + x_c = 1$), ρ is the number density, and $\phi_c = \pi\rho d_c^3 x_c/6$ is the particle volume fraction. Though the polymer volume fraction vanishes in this reference state, due to the absence of a core in the polymer–polymer interaction (see eq 9), the number density of the polymer is still important.

Radial Distribution Functions. Since the polymer has no hard core,

$$g^\circ_{pp}(r) = 1$$
$$g^\circ_{cp} = 0 \quad \text{for} \quad r < d_c/2$$
$$g^\circ_{cp} = 1 \quad \text{for} \quad r > d_c/2 \quad (12)$$

The particle radial distribution function, $g^\circ_{cc}(r)$, reduces to that for single-component hard spheres, which is difficult to obtain exactly, but the Percus Yevick approximation[19] provides results in good agreement with Monte Carlo calculations at low to moderate volume fractions. We adopt a numerical iteration procedure, developed by Perram,[21] to calculate $g^\circ_{cc}(r)$ and include the Verlet–Weis[22] correction, based on Monte Carlo simulations, to mitigate three inconsistencies at higher volume fractions: (1) values for $g^\circ_{cc}(r)$ are too small near the core; (2) the first maximum is too large; and (3) oscillations are slightly out of phase. The values before the correction are checked against Throop and Bearman's tabulations.[24]

Thermodynamics

Classical thermodynamics prescribes the relationships between the Helmholtz free energy and other macroscopic quantities such as pressure and chemical potential:

$$\mu_i = \partial A(T,V,N_1,N_2)/\partial N_i$$
$$P = -\partial A(T,V,N_1,N_2)/\partial V \quad (13)$$

Phase equilibrium in a binary mixture requires equality of pressure and of the chemical potential of each species in all phases.

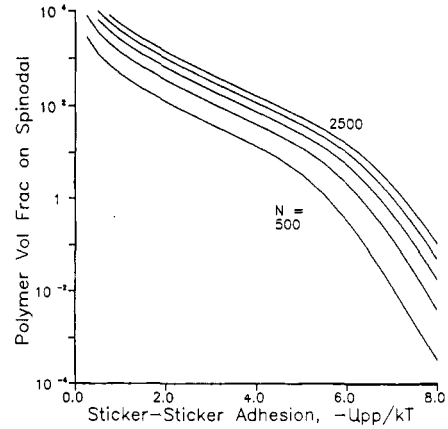

Figure 6. Polymer concentration at the limit of stability as a function of sticker–sticker adhesion for $N = 500$, 1000, 1500, 2000, and 2500. Concentrations to the right of a given curve are unstable.

Another important thermodynamic concept is that of stability.[21] A simple isolated system is in stable equilibrium at a maximum on the $S(U,V,N)$ surface or, equivalently, a minimum on the $U(S,V,N)$ surface. We can test the stability of a system by examining small perturbations, ΔS, from this maximum entropy equilibrium state. Such variations will increase the energy of the system and decrease its entropy according to

$$\Delta S = \delta S + \frac{1}{2!}\delta^2 S + \frac{1}{3!}\delta^3 S + \ldots + \frac{1}{m!}\delta^m S + \ldots \quad (14)$$

where the variations $\delta\mathbf{S}$ are, for example,

$$\delta S = (\partial S/\partial U)_{V,N_1,N_2}\delta U + (\partial S/\partial V)_{U,N_1,N_2}\delta V + (\partial S/\partial N_1)_{U,V,N_2}\delta N_1 + (\partial S/\partial N_2)_{U,V,N_1}\delta N_2 \quad (15)$$

If S varies smoothly, the maximum in S satisfies $\delta S = 0$ and $\delta^n S < 0$, where $\delta^n S$ is the lowest order nonvanishing variation. So the system is stable for $\delta^2 S < 0$ or $\delta^2 U > 0$. At the limit of stability, i.e., on the spinodal, these terms vanish, but $\delta^3 S < 0$. There are a number of equivalent ways to write this stability criterion. For example, for our binary system the determinants

$$L = \begin{vmatrix} A_{N_1N_1} & A_{N_1N_2} \\ A_{N_2N_1} & A_{N_2N_2} \end{vmatrix} \qquad M = \begin{vmatrix} A_{N_1N_1} & A_{N_1N_2} \\ L_{N_1} & L_{N_2} \end{vmatrix} \quad (16)$$

(subscript denotes partial derivative) must be positive if a point is stable but vanish at the critical point.

An important application of stability analysis is the determination of polymer solubility. For a single-component system of polymer molecules, the stability criteria determines the concentration beyond which no further polymer will dissolve. At the limit of stability,

$$dP/dV = 0 \quad (17)$$

When the compressibility is negative, the polymer solution becomes unstable. Figure 6 illustrates that stronger stickers destabilize polymer solutions, since solutions more concentrated than the spinodal are unstable. In other words, if the sticker–sticker adhesions are too strong, the polymer is insoluble. Experimentally, this means that associative thickeners are generally difficult to dissolve, despite their water-soluble backbones. In the concentration range of interest, $0 \leq \phi_p = 4\pi x_p \rho r_g^3/3 \leq 5$ ($r_g = lN^{1/2}/6^{1/2}$), sticker–sticker adhesions must not exceed 4–5kT. Note that this approach, which does not account for excluded volume, determines only the limit of polymer solubility, not the equilibrium polymer concentration in

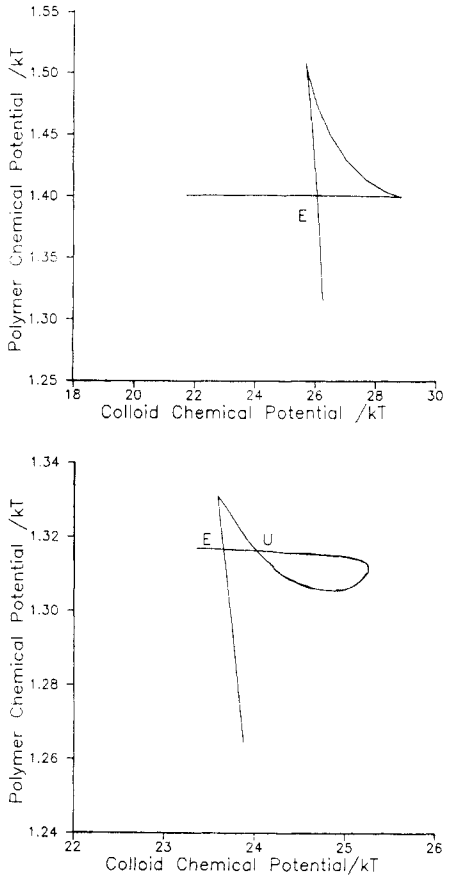

Figure 7. Isobars in chemical potential space for $d_c/2r_g = 2$, $N = 1000$. Point E is phase equilibrium; point U is unstable. (A, top) No attractive well in colloid–polymer potential: $u_{pp}/kT = -2$, $u_{pw}/kT = -1$. (B, bottom) Attractive well in colloid–polymer potential: $u_{pp}/kT = -1$, $u_{pw}/kT = -2.8$.

the solution. Thus, some of the concentrations to the left of the spinodal in Figure 4 may be supersaturated, i.e., metastable.

Procedure

We generate phase diagrams by determining the colloid and polymer concentrations for which the pressure and the chemical potentials of each species are equal in all phases. This requires calculating the pressure and chemical potentials for specific values of d_c/r_g, u_{pp}, u_{pw}, and N over a range of volume fractions of colloid and polymer. Our perturbation routines reproduce Melnyk and Sawford's calculations[13] of phase separation in systems of nonadditive hard spheres.

Phase diagrams are generated by a graphical rather than a numerical method. Newton–Raphson iteration fails because the surface that relates pressure and the two chemical potentials in μ_c–μ_p–P space has discontinuities of slope. For a given physical situation, i.e., u_{pp}, u_{pw}, and N fixed, phase diagrams are calculated one tie line at a time, each corresponding to an arbitrary pressure. The colloid volume fraction is varied over $0.01 \leq \phi_c \leq 0.5$ with sufficient polymer to maintain the pressure constant, generating an isobar in μ_c–μ_p space that may have either of the two characteristic shapes in Figure 7 for a phase-separated system.

In Figure 7A, the intersection of the line with itself identifies the equilibrium point; the compositions from the two branches of the isobar determine points on the equilibrium curve, connected by a tie line. Repeating the procedure with different pressures obtains sufficient tie lines to outline the phase envelope. Usually, tie lines are generated first for a high pressure (i.e., polymer concentration) to ensure phase separation, if at all possible. At lower pressures, the triangle in Figure 7A becomes smaller as the compositions of the two phases converge. At the critical point, the μ_c–μ_p isobar contains a kink, signifying that both phases have the same composition. In the one-phase region, smooth nonintersecting isobars are traced in the chemical potential plane.

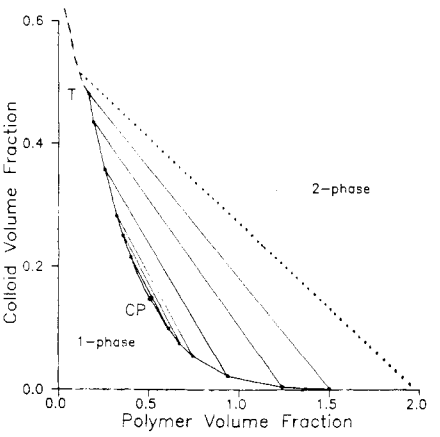

Figure 8. Typical phase diagram with tie lines shown. Critical point, CP. Dashed lines and T represent hypothetical solid line and triple point, respectively: $u_{pp} = u_{pw} = 0$, $N = 1000$, $d_c/2r_g = 2$.

Sometimes the isobars on the μ_c–μ_p plots intersect themselves twice, as Figure 7B depicts. A stability analysis, based on eq 16, shows that point U is unstable, leaving E as the true equilibrium point. Note that systems with two intersections do not reach a critical point. As pressure is lowered, the loop becomes smaller and eventually the curve intersects itself at a tangency point, indicating the phase diagram ends in a tie line rather than a critical point. The thermodynamic significance of this behavior remains unclear.

Figure 8 shows a phase diagram of type A, which contains a critical point. The vertical axis measures the volume fraction of particles while the horizontal axis shows the volume fraction of the polymer, based on the radius of gyration. Because polymer molecules can interpenetrate, the latter may exceed unity. The two-phase region lies to the right of the curve, as indicated by the tie lines. To use a phase diagram, one locates the initial state of the system by finding the point corresponding to the total volume fractions of particles and polymer. If this point lies in the two-phase region, the ends of the tie line give the equilibrium compositions of the two phases and the inverse lever arm rule determines the amount of each phase present. This phase diagram shows only a fluid–fluid transition; a fluid–solid transition is also possible and is quite likely for $\phi_c > 0.5$. The dashed and dotted lines anticipate the shape of such a phase diagram. The dashed line represents a solid state, dense with particles and containing little polymer, in equilibrium with a concentrated polymer solution, as indicated by the dotted line. T is the anticipated triple point where the solid and both dense and dilute fluid phases equilibrate.

The next section discusses sets of phase diagrams with varying u_{pp}, u_{pw}, and N to illustrate the effects of associating polymer on the colloidal dispersion. For simplicity, most tie lines and critical point are omitted from these graphs.

Results and Discussion

Figure 9 displays a family of equilibrium curves that illustrate the effects of sticker–colloid adhesion on the phase behavior of the binary system. Here polymer size

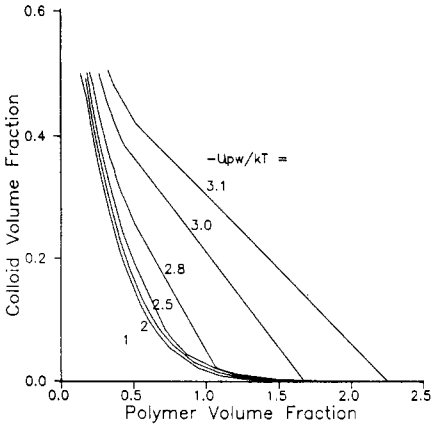

Figure 9. Effect of sticker–colloid adhesion on phase behavior: colloid volume fraction versus polymer volume fraction based on r_g, $N = 1000$, $d_c/2r_g = 2$, and $u_{pp}/kT = -1$. There is no critical point for $-u_{pw}/kT = 2.5$, 2.8, 3.0, and 3.1.

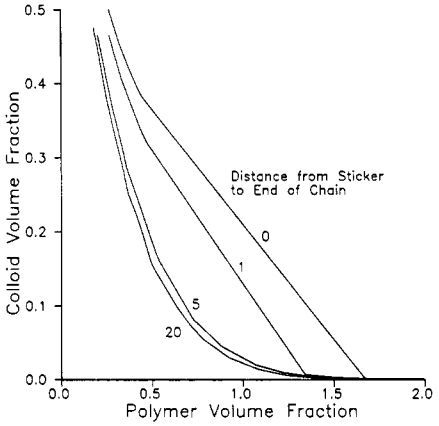

Figure 10. Effect of sticker position on phase behavior: colloid volume fraction versus polymer volume fraction based on r_g, $N = 1000$, $d_c/2r_g = 2$, $u_{pw} = -3kT$, and $u_{pp} = -kT$.

and sticker–sticker adhesion are held constant at $N = 1000$ and $u_{pp} = -kT$. The curves shift to the right as the polymer–colloid adhesion grows stronger, indicating that more polymer is required to induce phase separation. A second and more marked effect appears as the polymer–colloid adhesion becomes stronger; the phase transition shifts from type A to type B in Figure 7. The two-phase region ends abruptly at the leftmost tie line. For $-u_{pw} > 2.7kT$ there is no critical point. Indeed, the critical point is generally absent in phase diagrams of systems whose colloid–polymer interaction has an attractive well. As we anticipated from the form of the pair potentials, polymer–colloid attraction suppresses the tendency to phase separate.

For systems with large sticker–wall adhesions, such as $-3.1kT$ where the last tie line ends at a volume fraction of $\phi_c = 0.5$, the fluid–fluid transition may be superceded by a fluid–solid transition, which has not been calculated. This last fluid–fluid point may fall beyond the triple point, so that the fluid–fluid transition would not be observed.

Figure 3 demonstrates that moving the stickers away from the ends of the chain has the same effect on the polymer–particle potential as decreasing the sticker–wall adhesion (Figure 2). We anticipate similar trends in phase behavior. Figure 10 illustrates that a system stabilized against volume restriction flocculation by a $-3kT$ sticker–wall adhesion will separate as the stickers move toward the center of the backbone. As few as 20 segments between the sticker and the end of the chain can mask the sticker completely, causing the same phase behavior predicted in the absence of stickers.

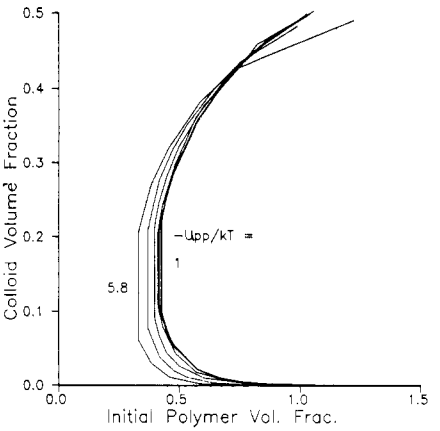

Figure 11. Effect of sticker–sticker adhesion and initial polymer volume fraction on the solids content of the resulting phases for initial solids content $\phi_c = 0.2$. Colloid volume fraction in heavy and light phases is shown as a function of initial polymer volume fraction in fluid. $N = 1000$. $u_{pw}/kT = -1$. $d_c/2r_g = 2$. $-u_{pp}/kT = 1.0$, 2.0, 3.0, 4.0, 5.0, 5.5, and 5.8.

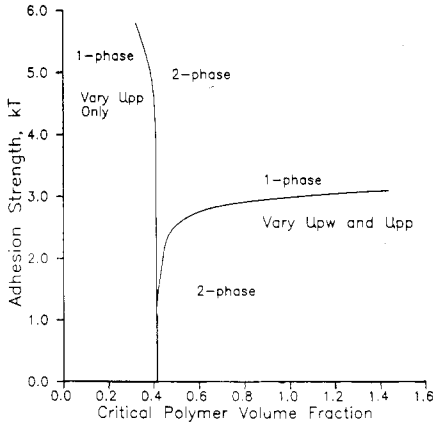

Figure 12. Minimum polymer needed to flocculate a system containing a total of $\phi_c = 0.2$. $N = 1000$. $d_c/2r_g = 2$. On leftmost curve, $u_{pw}/kT = 0$ and u_{pp}/kT varies along the vertical axis. On right curve, $u_{pp}/kT = u_{pw}/kT$, as shown on vertical axis.

Figure 11 depicts an alternate representation of sets of equilibrium curves for comparison with experiments in which only the particle compositions of the separated phases are measured. In contrast to the previous type of phase diagrams, the horizontal axis shows the polymer volume fraction of the original solution, rather than the polymer content of the resulting phases. Thus, the tie lines are always vertical. The phase boundary of this diagram depends on the initial particle volume fraction. Indeed, a different phase diagram must be generated for each initial volume fraction of colloids. Those systems initially containing the same solids fraction as the critical point will yield smooth phase diagrams that show the critical point as the leftmost point. Any system with a different solids content will generate a curve that ends abruptly at the left in a tie line, an artifact of the representation rather than an indication of the absence of a critical point.

Figure 11 shows the effects of sticker–sticker adhesion on the phase behavior of a system initially containing $\phi_c = 0.2$ solids with $N = 1000$ and $u_{pw} = -kT$. Stronger sticker–sticker adhesions destabilize the system, as suggested by the interaction potentials in the previous section. Recall that the magnitude of the sticker–sticker adhesion cannot exceed $5kT$ without destabilizing the polymer solution.

Important quantities for formulating polymer-containing dispersions are (a) the amount of polymer that can be tolerated before a system phase separates and (b) the

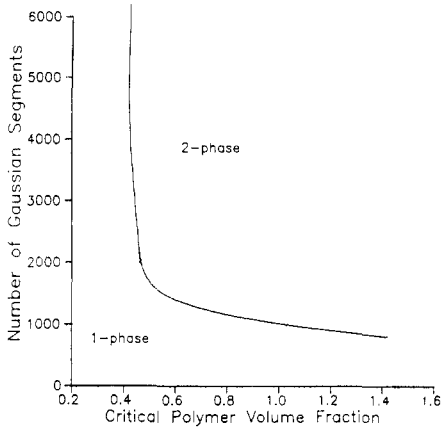

Figure 13. Minimum polymer needed to flocculate a system containing a total of $\phi_c = 0.2$ as a function of polymer flexibility (N) with $d_c/2r_g = 2$, $u_{pw}/kT = -3.0$, and $u_{pp}/kT = -1.0$.

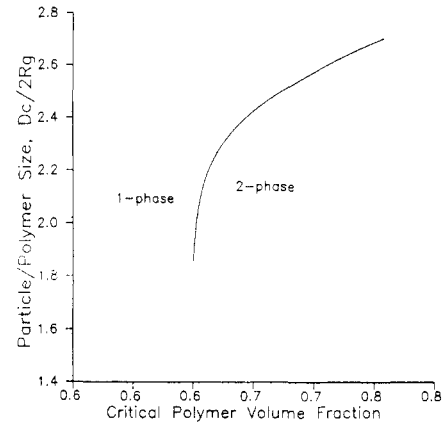

Figure 14. Minimum polymer needed to flocculate a system containing a total of $\phi_c = 0.2$ with varying particle size. $N = 1000$, $u_{pw} = -2.8kT$, and $u_{pp} = -kT$.

strength of the associations needed to stabilize a system that would otherwise separate. Figure 12, a condensed type of phase diagram, illustrates how these quantities depend on polymer characteristics in systems initially containing $\phi_c = 0.2$ with $N = 1000$. The sticker–sticker or sticker–wall adhesion is shown on the vertical axis, while the horizontal axis contains the crucial information: the amount of polymer which induces phase separation. There are two branches. The rightmost branch shows the critical polymer concentration as a function of $u_{pp} = u_{pw}$. The leftmost branch pertains to variations in u_{pp} with $u_{pw} = 0$. The region where both branches of the curve join to intersect the horizontal axis at $\phi_p = 0.43$ signifies the polymer required to destabilize the system in the absence of stickers—presumably by volume restriction flocculation.[4,11,12] Increasing the sticker–wall adhesion stabilizes the system, while increasing the sticker–sticker adhesion ultimately destabilizes the system at very strong sticker–sticker adhesions.

A similar type of condensed phase diagram (Figure 13) shows the effects of chain flexibility with $u_{pw} = -3.0kT$ and $u_{pp} = -kT$. Flexibility is varied by changing N, while maintaining a constant polymer/colloid diameter ratio by adjusting the segment length. Increasing flexibility destabilizes the system. We attribute this to the decrease in particle–polymer attraction with increasing N (Figure 5), presumably because more segments obscure the effects of the stickers. Not evident in Figure 13 is the loss of the critical point for polymers with $N \leq 1400$, consistent with the appearance of an attraction in the polymer–colloid potential. Note that, for very flexible polymers, the amount of polymer necessary to induce flocculation is the same as that in the weak sticker limit of Figure 12.

Testing the effect of polymer size is limited by the assumption that the colloid must be significantly larger than the polymer. This assumption should be reasonable for the cases examined here with $d_c/2r_g = 2$. For small particle sizes, it is difficult to judge in which direction the model would err. When curvature is important, the model overpredicts both the probability of stickers encountering the surface, favoring stabilization, and the loss of configurational entropy of the polymer, favoring separation. Increasing the particle size stabilizes the system against fluid–fluid separation (Figure 14), but the current theory does not predict the ensuing fluid–solid transition.

The excluded volume interactions between polymer segments neglected by this model would introduce a repulsive core to the polymer–polymer interaction potential, resulting in lower polymer solubility, and a longer range repulsion in the polymer–particle potential, which favors volume restriction flocculation. Thus, we speculate that stronger sticker–wall adhesion strengths would be required to stabilize the system against volume restriction flocculation in the presence of significant excluded volume interactions.

Conclusions

A statistical treatment of a Gaussian polymer with adhesive end groups provides polymer–polymer and polymer–particle pair potentials. Incorporation of these into an appropriate statistical mechanical model then predicts the phase behavior of dispersions. The limiting assumptions are that (a) excluded volume interactions are neglected, (b) the polymer must be significantly smaller than a particle, and (c) hydrophobic end groups have negligible volume. Our technique predicts the minimum polymer volume fraction that will induce a fluid–fluid phase separation and the compositions of the resulting phases, given an initial set of parameters. The model predicts fluid–fluid phase separations for systems whose equivalent hard sphere diameters are significantly nonadditive and for systems where the polymer–polymer potential is strongly attractive. As anticipated, strong ($\leq -2.5kT$) sticker–particle adhesion stabilizes the system, overcoming the effects of nonadditivity and polymer–polymer attraction. Placing the sticker on the end of the chain ensures the strongest influence on phase behavior. In systems with strong sticker–particle interaction, a fluid–solid transition may preclude the fluid–fluid phase separation. The nature of the polymer backbone is as important as the sticker strengths. With large or flexible polymers, entropic effects dominate the adhesion of the stickers to destabilize the system. When the polymer is stiff, the stickers strongly influence phase behavior.

These results await quantitative experimental confirmation, though similar behavior has been observed.[3] Future work also includes modeling the system in such a way that segment–segment interactions limit the surface coverage of the particles and influence solution properties. Hopefully, this approach will facilitate the prediction of bridging flocculation and fluid–solid equilibrium.

Acknowledgment. This research was funded by a grant from Hercules/Aqualon and a National Science Foundation Fellowship to M. M. Santore.

References and Notes

(1) Vincent, B.; Luckham, P. F.; Waite, F. A. *J. Colloid Int. Sci.* **1980**, *13*, 508.
(2) Healy, T. W.; La Mer, V. K. *J. Phys. Chem.* **1962**, *66*, 1835.
(3) Sperry, P. R.; Thibeault, J. C.; Kostansek, E. C. *Adv. Org. Coat. Sci. Technol.* **1985**, *9*, 1.

(4) Gast, A. P.; Russel, W. B.; Hall, C. K. *J. Colloid Int. Sci.* **1986**, *76*, 189.
(5) Vrij, A. *Pure Appl. Chem.* **1976**, *48*, 471.
(6) Glass, J. E. *Adv. Chem. Ser.* **1986**, *213*, 391.
(7) Gelman, R. A.; Barth, H. G. *Adv. Chem. Ser.* **1986**, *213*, 101.
(8) Sperry, P. R.; Hopfenberg, H. B.; Thomas, N. L. *J. Colloid Int. Sci.* **1981**, *82*, 62.
(9) US Patent 4,079,029, 1978.
(10) Sperry, P. R. *J. Colloid Int. Sci.* **1984**, *99*, 97.
(11) Gast, A. P.; Hall, C. K.; Russel, W. B. *J. Colloid Int. Sci.* **1983**, *96*, 251.
(12) Gast, A. P.; Hall, C. K.; Russel, W. B. *Faraday Chem. Soc. Discuss.* **1983**, *76*, 189.
(13) Melnyk, T. W.; Sawford, B. L. *Mol. Phys.* **1975**, *29*, 891.
(14) Cates, M. E.; Witten, T. A. *Macromolecules* **1986**, *19*, 732.
(15) Henderson, D.; Barker, J. A. *J. Chem. Phys.* **1968**, *49*, 3377.
(16) Henderson, D.; Leonard, P. J. *Phys. Chem: Adv. Treatise* **1971**, *8*, 413.
(17) Flory, P. J. *Principles of Polymer Chemistry*; Cornell University Press: Ithaca, NY, 1953; p 402.
(18) Casassa, E. F. *Sep. Sci.* **1971**, *6*, 305.
(19) McQuarrie, D. A. *Statistical Mechanics*; Harper and Row: New York, 1973; p 203.
(20) Mansoori, G. A.; Carnahan, N. F.; Starling, K. E.; Leland, T. W. *J. Chem. Phys.* **1971**, *54*, 1523.
(21) Perram, P. W. *Mol. Phys.* **1975**, *30*, 1505.
(22) Verlet, L.; Weis, J. J. *Phys. Rev. A* **1972**, *5*, 939.
(23) Modell, M.; Reid, R. C. *Thermodynamics and Its Applications*, 2 ed.; Prentice Hall: Englewood Cliffs, NJ, 1983; p 227.
(24) Throop, G. J.; Bearman, R. J. *J. Chem. Phys.* **1965**, *42*, 2408.

Temperature Dependence of the Phase Equilibria for the System Poly(ethylene glycol)/Dextran/Water. A Theoretical and Experimental Study

Åke Sjöberg*,†,‡ and Gunnar Karlström§

Departments of Physical Chemistry 1 and Theoretical Chemistry, Chemical Centre, P.O. Box 124, S-221 00 Lund, Sweden. *Received April 20, 1988; Revised Manuscript Received August 19, 1988*

ABSTRACT: A new mean field theory, based on the Flory–Huggins description of polymer solutions, is used to describe the temperature dependence of the phase diagram for the ternary poly(ethylene glycol)/dextran/water system. The use of this model gives a great improvement compared to the use of the conventional Flory–Huggins theory. For a fixed set of monomer interaction energies the model is able to reproduce our experimental observations for the PEG20000/Dextran(T40)/water system almost quantitatively up to 80 °C and is qualitatively correct at even higher temperatures. In both model calculations and experiments we found, at temperatures comparable to the cloud point of the poly(ethylene glycol), a three-phase area that has not been reported previously. Finally, a new interpretation for the clear solutions observed previously in the two-phase region of the phase diagram at 95 °C is given.

Introduction

The phase separation occurring when a system consisting of a solvent and two polymers separates into two isotropic polymer phases with mainly one polymer in each phase is a since long-known general phenomenon in both aqueous and organic solvents. During the last 30 years the partitioning of biological macromolecules in aqueous two-phase systems has been developed into a very powerful unit operation for enzyme and protein purification in the biochemical laboratory.[1,2] By far the most used systems for this purpose are those composed of poly(ethylene glycol), dextran, and water.

Even though a tremendous empirical know-how in using aqueous two-phase systems for partitioning purposes has been built up during these 30 years, there do not exist many studies of the fundamental physicochemical aspects of phase separation in aqueous two-polymer systems. Today, when different groups all over the world try to develop aqueous two-phase partitioning to a useful full-scale unit operation in the biotechnical industry,[3-7] the value of such fundamental studies has increased both for designing totally new two-phase systems and for optimizing already existing phase systems.

In a previous paper[8] one of us has concluded that the mechanism leading to phase separation in aqueous polymer systems has the same origin as that for polymers in organic solvents. This means that the explanation to phase separation is not to be found in some specific property of the solvent but is rather to be found in the molecular interactions between the different polymer components. As was shown[8] phase separation in aqueous polymer systems can be analyzed in terms of classical Flory–Huggins theory for a polymer 1/polymer 2/solvent system.

In this work we will study the temperature dependence of the phase equilibria in the poly(ethylene glycol)/dextran/water system by experimental and theoretical investigations and thereby get a deeper insight in the molecular interactions leading to phase separation.

Since classical Flory–Huggins theory, with temperature-independent interaction parameters, cannot describe the temperature dependence for the binary poly(ethylene glycol)/water system, we treat the poly(ethylene glycol) along the lines proposed by Karlström,[9] which leads to a somewhat different treatment compared to Scott's[10] treatment of a polymer 1/polymer 2/solvent system.

With this new model, the theoretical description of the poly(ethylene glycol)/dextran/water system has been greatly improved relative to a conventional Flory–Huggins description. The model calculations can predict the decreased solubility above 90 °C. In this model phase separation at low and moderate temperatures is due to poly(ethylene glycol)–dextran interactions, and at temperatures above ≈90 °C the phase separation is also due to poly(ethylene glycol)–water interactions.

In the experimental section phase diagrams for the system poly(ethylene glycol)/dextran/water are given at

† Previously Åke Gustafsson.
‡ Department of Physical Chemistry 1.
§ Department of Theoretical Chemistry.

0024-9297/89/2222-1325$01.50/0